European Journal of Medicinal Chemistry 48 (2012) 124–131

Contents lists available at SciVerse ScienceDirect

European Journal of Medicinal Chemistry

journal homepage: http://www.elsevier.com/locate/ejmech

Original article

Design, synthesis and biological evaluation of new naphtalene diimides bearing isothiocyanate functionality

Anna Minarini [a,*], Andrea Milelli [a], Vincenzo Tumiatti [a], Lorenzo Ferruzzi [b], Melinda-Rita Marton [c], Eleonora Turrini [b], Patrizia Hrelia [b], Carmela Fimognari [b]

[a] Dipartimento di Scienze Farmaceutiche, Alma Mater Studiorum, Università di Bologna, Via Belmeloro 6, 40126 Bologna, Italy
[b] Dipartimento di Farmacologia, Alma Mater Studiorum, Università di Bologna, via Irnerio 48, 40126 Bologna, Italy
[c] Chemical Engineering Department, University Politehnica of Bucharest, RO-011061 Polizu 1-7 Bucharest, Romania

ARTICLE INFO

Article history:
Received 21 September 2011
Received in revised form
28 November 2011
Accepted 3 December 2011
Available online 8 December 2011

Keywords:
Sulforaphane
Anticancer
Isothiocyanates
Naphthalene diimides
Multi-target-directed ligands

ABSTRACT

The synthesis and the biological activities of new derivatives **1**–**3**, characterized by the isothiocyanate (ITC) functionalities coming from sulforaphane (SFN), a well-known anticancer natural product, were reported. The most interesting compound of the series was **2**. It was chemically characterized by two ITC functionalities mounted on the 1,4,5,8-naphthalentetracarboxylic diimide (NDI) scaffold through two polymethylene chains, each constituted by three carbon units. It demonstrated an IC_{50} value in the submicromolar range, more potent than SFN, displaying also the ability to trigger apoptotic induction in the same range by eliciting both extrinsic and intrinsic apoptotic pathways. Finally, it was observed that **2** inhibited the cell growth by blocking the cell cycle in G1 phase.

1. Introduction

Novel chemotherapeutic agents and new strategies for cancer treatment represent active research fields stimulated by the discovery of both new biological targets and drugs without serious side effects [1]. Furthermore, there is a common acceptance that drugs able to hit multiple cancer targets seem to be more adequate for the treatment of cancer, which involves multiple pathogenic factors, in comparison with those modulating only one target. These new agents were defined as Multi-target-directed ligands (MTDLs) [2–4].

Several anticancer agents recently published in literature are characterized by Naphtalene diimide (NDI) scaffold especially those interacting with DNA as intercalators [5–9] and many reviews were published on these aspects [7,8]. In particular, several derivatives characterized by NDI scaffold have been reported able to exhibit bis-threading intercalating ability [10], to enhance the stabilization of DNA triplexes [11], to stabilize [12] or alkylate [13] G-quadruplex DNA structure [14]. Finally, it is to note that an NDI derivative able to inhibit telomerase activity represents a new approach for the treatment of human gastrointestinal stromal cancer which developed resistant mutations in the kinase active site [15].

One of the main prototype of NDI derivatives is represented by N-BDMPrNDI (Fig. 1) which showed the ability to intercalate into steps containing at least one G:C base pair [16]. Recently, we have published a paper in which we reported a new series of Naphthalene imide (NI) and NDI derivatives as antiproliferative agents [17]. The most cytotoxic compound was characterized by NDI scaffold suitable decorated with two basic chains constituted by three methylene units of length bearing a 2-methoxybenylamino moiety and endowed with an interesting biological profile [18].

In order to search new anticancer agents characterized by a MTDLs biological profile, we explored the possibility to insert on the NDI scaffold other functionalities deriving from the natural kingdom and already known for their anticancer properties, such as the isothiocyanate (ITC) one. Different widely consumed vegetables contain ITCs, such as watercress, broccoli, cabbage, and cauliflower, sharing this function stored as glucosinolates, and exert chemopreventive and therapeutic anticancer activities [19–22]. A complete overview about the ITC's chemopreventive mechanisms was reported by Keum and coll [23]. Sulforaphane (SFN) (Fig. 1), one

Abbreviations: NI, naphthalimmide; NDI, 1,4,5,8-naphthalenetetracarboxylic diimide; MTDL, Multi-target-directed ligands; ITC, isothiocyanate; SFN, sulforaphane.

* Corresponding author. Tel.: +39 051 2099709; fax: +39 051247600.
E-mail address: anna.minarini@unibo.it (A. Minarini).

0223-5234/$ – see front matter © 2011 Elsevier Masson SAS. All rights reserved.
doi:10.1016/j.ejmech.2011.12.003

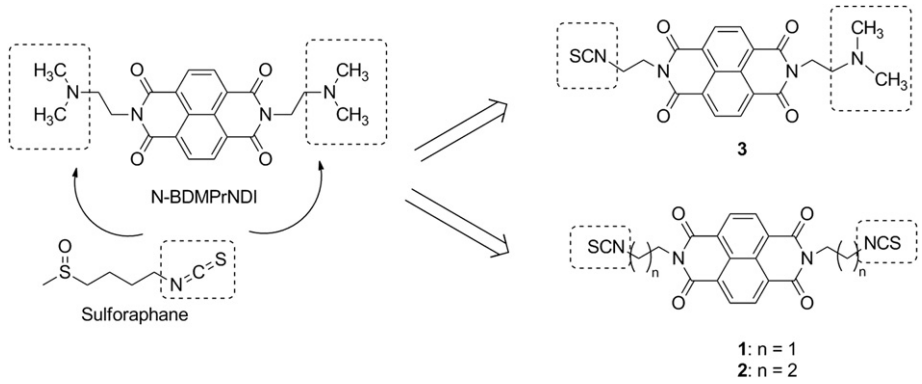

Fig. 1. Chemical structures of N-BDMPrNDI, sulforaphane, and drug design of **1**–**3**.

of the most widely investigated ITCs, was effective to prevent and to treat different cancer types [24]. In particular, it showed the ability to modulate cell cycle and apoptosis [25], to increase the efficacy of doxorubicin [26], to induce DNA single strand breaks [27], to interfere with all essential steps of neovascularization [28], and to inhibit the metastatic potential of cancer cells [29].

On these bases we decided to incorporate the ITC group (–N=C=S) in the NDI scaffold by replacing the two basic functions of N-BDMPrNDI with the ITC groups and by varying the side chains length from 2 to 3 methylene units, providing **1** and **2**, respectively (Fig. 1). The choice of these two different lengths was based on a previous paper in which we described several NDI derivatives with chains varying from two to ten methylene units. Among them the most potent compounds were those characterized by two and three methylene side chains [17].

Furthermore, to evaluate the importance of the number of the ITC functions, derivative **3** was designed. This compound is characterized by an asymmetric structure constituted by two different side chains, one bearing a protonated dimethylaminoethyl side chain deriving from N-BDMPrNDI, and the second one characterized by the ITC group.

During the drafting of the present paper Sharma and coll. published an interesting study in which they applied the same strategy reported above on NI scaffold, discovering a very promising compound as potential melanoma therapeutic characterized by an ITC group mounted on a side chain of two methylene units [30]. Their interesting results strengthened the robustness of the rationale of the present investigation, considering that we explored and expanded this principle by introducing the ITC group on NDI scaffold. Finally, it is worth to note that an additional aspect of novelty is constituted by the design and synthesis of the asymmetric derivative **3**. In fact, a limited number of such asymmetric derivatives with NDI scaffold have been reported in literature so far.

2. Results and discussion

2.1. Chemistry

Compounds **1** and **2** were synthesized following the procedure reported in Scheme 1. Compounds **4** and **5** [17] were reacted with commercially available 1,1′-thiocarbonyldi-2(1H)-pyridone [31] to provide the corresponding isothiocyanates **1** and **2**.

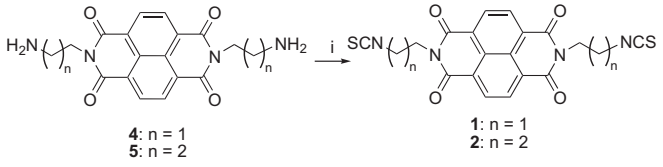

Scheme 1. Reagents and conditions: (i) 1,1′-thiocarbonyldi-2(1H)-pyridone, CH_2Cl_2, room temp., overnight, 41–48% yields.

The synthesis of compound **3** is reported in Scheme 2. Naphthalene-tetracarboxylic dianhydride, mono-Boc-protected diaminoethane [32] and *N*,*N*-dimethylethylenediamine were condensed in order to provide **6**; removal of the Boc protecting group through acidic hydrolysis led to **7** which was reacted with 1,1′-thiocarbonyldi-2(1H)-pyridone to provide the corresponding asymmetric isothiocyanate **3**.

2.2. Biological evaluations

2.2.1. Cytotoxic and cytostatic activity in vitro

Derivatives **1**–**3** were preliminary evaluated in *in vitro* assays for their cytotoxic and cytostatic effects on a human T lymphoblastoid cell line (Jurkat) (Fig. 2). Jurkat T leukemia cells were treated for 24 h with various concentrations (0.0–16.0 μM) of each compound. A dose-dependent decrease in cell viability was observed for all the compounds (Fig. 2). Due to the instability of **1**–**3** towards nucleophiles, a longer exposure to these compounds (72 h) induced a high fraction of necrotic cells. As an example, at the concentration 1 μM, the percentage of necrotic cells was 100% for all three compounds. This might suggest that longer times of exposure can cause some forms of intensive cell toxicity.

The reference compound N-BDMPrNDI exhibited an IC_{50} of 3.43 μM, while **1**–**3** showed a cytotoxic potency that was consistently higher than that observed for N-BDMPrNDI. We indeed recorded the following IC_{50} (μM) values: 0.89 for **1**, 0.43 for **2**, and 1.91 for **3**. The dose required to reach IC_{50} for SFN, the most studied

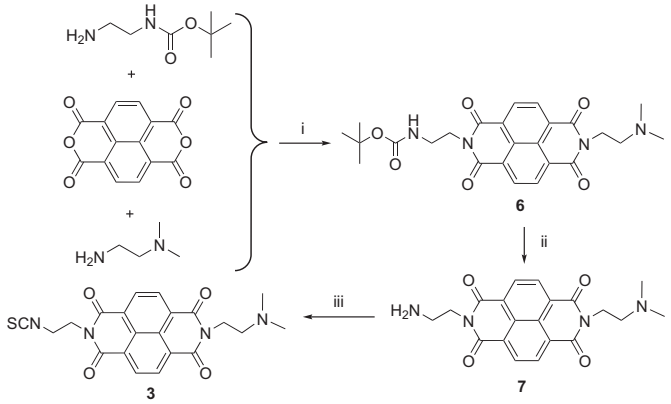

Scheme 2. Reagents and conditions: (i) DMF, reflux, 2 h, 15%; (ii) HCl 3 N, MeOH, room temp. overnight, quantitative yield; (iii) 1,1′-thiocarbonyldi-2(1H)-pyridone, CH_2Cl_2, room temp., overnight, 45% yield.

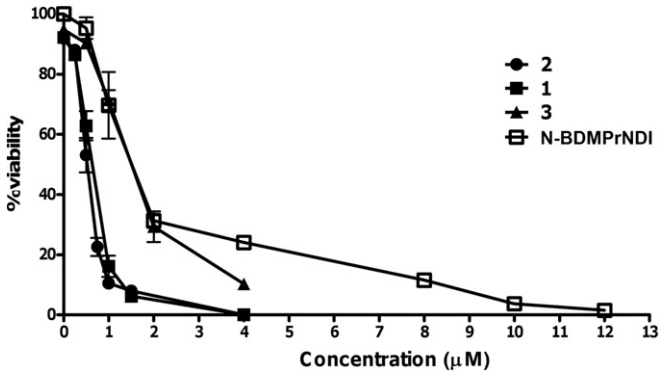

Fig. 2. Cytotoxicity of **1**–**3** and reference compound N-BDMPrNDI against Jurkat T leukemia cells after 24 h of compounds exposure. Data are means ± SEM of at least three independent experiments.

natural ITC, in the same cell line (15 μM) [24] was about 17-, 35- and 8-fold higher than that recorded for **1**–**3**, respectively. The data related to **1**–**3** could be merely rationalized in terms of lipophilicity, taking into account that **2** is characterized by the highest value of ClogP of the series (data not shown).

2.2.2. Apoptosis triggering

After these first screening assays, **1**–**3** were further investigated to determine their cytotoxic and cytostatic molecular mechanisms. In fact, as reported for ITCs, the new compounds could exert their cytotoxic effect by multiple independent mechanisms. First, we determined whether **1**–**3** caused the activation of apoptosis and/or necrosis. To this end, Jurkat cells were treated with the three compounds for 24 h, followed by the assessment of the exposure of phosphatidylserine by using Guava Nexin Reagent. The early exposure of phosphatidylserine increased in a dose-dependent manner and was associated with the increased number of cells committed to apoptosis observed for all the compounds (Fig. 3). It is worth noting that their proapoptotic potency was similar for **1** and **3** (Fig. 3B and C) or even higher for **2** (Fig. 3A) than that reported for the cytotoxic drug camptothecin, as positive control. At higher concentrations, all the compounds induced necrosis (Fig. 3), as revealed by the number of cells permeable to a vital dye such as 7-amino-actinomycin. The proapoptotic potential of **1**–**3** was similar or even higher than that demonstrated by SFN (Fig. 3). Of additional interest is the recognition that the concentration of SFN able to increase the fraction of apoptotic cells is about 40-fold higher than that of **2** (30 μM *vs* 0.75 μM).

Apoptosis is primarily mediated through two pathways: the death receptor pathway and the mitochondrial pathway. In the first one, a death receptor ligand, such as Fas ligand, binds to its receptor, such as Fas, triggering aggregation of the death receptor, recruitment of an adaptor molecule, such as FADD, as well as pro-caspase-8 or -10 forming a complex named the death inducing signalling complex. These results in the autocatalytic cleavage and activation of caspase-8 or caspase-10, leading to induction of apoptosis [33]. In the mitochondrial pathway, multidomain proapoptotic proteins, excessive mitochondrial calcium and reactive oxygen species induce the opening of the mitochondrial pore, with loss of mitochondrial integrity and transmembrane potential ($\Delta\Psi$m) [34]. Thus, for the specific measurement of $\Delta\Psi$m, Jurkat cells were loaded with the fluorochrome JC-1, a cationic probe that distributes passively between media, the cytosol and the mitochondria according to the Nernst's equation, where the final distribution of the fluorochrome depends mainly on the transmembrane potential [35]. Normal cells exhibited a mitochondrial transmembrane

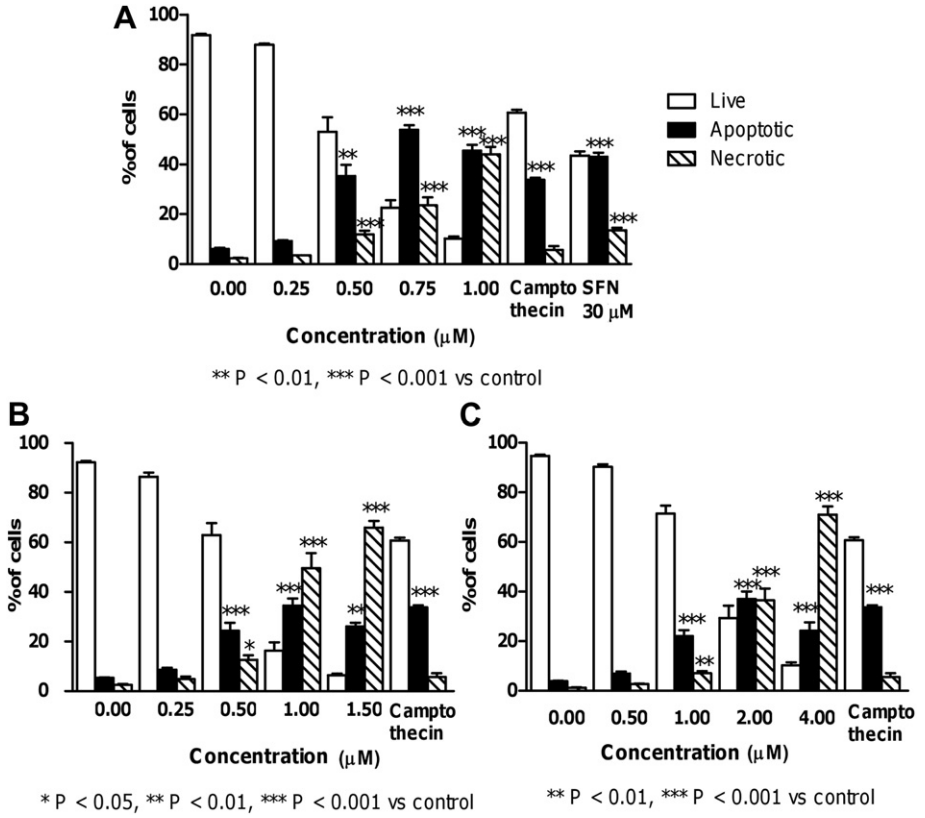

Fig. 3. Activation of apoptosis and/or necrosis by **2** (A), **1** (B), **3** (C) in comparison with camptothecin (2 μM) and SFN (30 μM). Data are means ± SEM of at least three independent experiments.

potential resulting from the asymmetric distribution of protons and other ions on both sides of the inner mitochondrial membrane. Compared to control cells, **1**–**3** treated cells had drop in $\Delta\Psi m$ (Fig. 4).

The fraction of cells with decreased mitochondrial potential reached around 50% at 0.50 μM for **1** and **2** (50.6% ± 6.6 and 47.1% ± 4.8, respectively) and 1.00 μM for **3** (53.0% ± 5.0). At the highest concentration tested, the number of cells with decreased mitochondrial potential was around 100%. The death receptor pathway was also induced by the investigated compounds, as indicated by the activation of caspase-8 (Fig. 5). The percentage of activated caspase-8 cells in not treated cultures was about 5%, which was increased up to 66% in cells treated with **1**, 68% in cells treated with **2**, and 56% in cultures treated with **3** at the highest concentrations tested (Fig. 5).

Both the loss of $\Delta\Psi m$ and the activation of caspase activity increased in a dose-dependent manner. Mutations in genes involved in the regulation of the mitochondrial pathway are very common in cancer cells. As the majority of anticancer therapies induce apoptosis in cancer cells by triggering the intrinsic pathway, such mutations are usually associated with treatment resistance. On the other hand, surface expression of death receptors may vary between different cell types and can be downregulated or absent in resistant forms of tumours [36]. Based on these observations, the ability of **1**–**3** to elicit both apoptotic pathways is particularly interesting and should be considered for further investigations.

2.2.3. Cell-cycle growth and distribution

We further investigated the ability of **1**–**3** to inhibit cell growth. **2** significantly suppressed the progression of cells into the cell cycle (Fig. 6A). At 0.75 μM, **2** suppressed Jurkat growth by about 30% and at 1.00 μM by 65%. At 2.00 μM, cell growth was almost completely suppressed. Similar results were recorded for **1** (Fig. 6B). At 1.00 μM, it inhibited cell growth by about 40%, at 1.50 μM by 58% and at 3.00 μM by 94%. The effect of **3** on cell growth was slightly less potent than **1** and **2** (Fig. 6C). **3** reduced Jurkat growth by 30% at 2 μM, 40% at 4 μM and 90% at 8 μM.

We then examined the effect of the three ITCs on cell-cycle distribution. According to our flow cytometry data, treatment of Jurkat cells with **2** resulted in a significant inhibition of cell growth, due to the block of cells in the G_1 phase (Fig. 7A).

The effect appeared primarily as a significant increase in the proportion of cells in the G_1 phase of the cell cycle (from about 56% to 68%) accompanied by a slight compensatory decrease in S (from about 21% to 13%) and G_2/M phase cells (from 29% to 22%) (Fig. 7A). Jurkat exposure to **1** similarly led to a decrease in the proportion of S and G_2/M cells, while the percentage of cells in G_1 phase increased from 58% to 68% (Fig. 7B). Cell treatment with **3** induced an increase in G_1 phase cells (from 63% to 68%), an unaffected fraction of G_2/M phase cells and a slight reduction in the proportion of S cells (from 20% to 15%) (Fig. 7C).

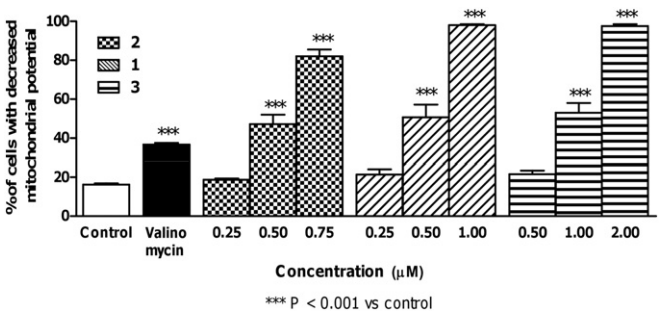

Fig. 4. Fraction of cells with decreased mitochondrial potential after treatment with **1**, **2** or **3**, in comparison with valinomycin. Data are means ± SEM of at least three independent experiments.

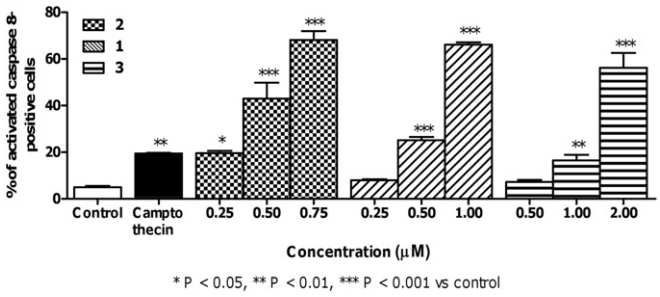

Fig. 5. Activation of caspase-8 following treatment with **1**, **2** or **3** for 24 h. Data are means ± SEM of at least three independent experiments.

Altogether these data demonstrated that these new synthesized ITCs, characterized by the presence of a NDI scaffold, are able to induce cell cycle inhibition or apoptosis in a leukemic cell line. These observations imply that the growth inhibition of Jurkat cells produced by **1**–**3** results from a combination of apoptosis and of cell-cycle derangements in which G_1 inhibition is a key event. Bearing in mind that G_1 regulation is frequently lost in human cancer [37] and that the product of the retinoblastoma susceptibility gene, Rb, is involved in G_1 transition and represents the focal point of an axis that is universally disrupted in human cancer [38], the ability of **1**–**3** to inhibit the cell cycle at G_1 phase is particularly interesting and warrants further investigations.

Finally, the simultaneous appearance of G_1 inhibition and apoptosis clearly indicates that cell death is a primary direct effect due to the tested compounds, and not to activation of apoptotic pathways as a consequence of cells' inability to overcome growth arrest and proceed through the cell cycle.

3. Conclusions

The introduction of chemical functionalities deriving from the natural kingdom may represent a new strategy to search new MTDLs, able to hit simultaneously the different biological targets peculiar of cancer pathology. In the present paper the synthesis and the biological characterization of new NDI derivatives **1**–**3**, endowed with ITC functionalities deriving from SFN, a well-known anticancer natural product, were reported. Their interesting biological profiles supported the validity of this approach. A simplified scheme of the multiple molecular targets involved in their anticancer activities is reported in Fig. 8. The most interesting compound of the series was **2**, chemically characterized by two ITC functionalities mounted on the NDI scaffold through two polymethylene chains constituted by three carbon units. To note that the most interesting biological data are related to **1** and **2**, characterized by two ITC groups, in comparison with **3** characterized by only one ITC group, supporting the hypothesis that two ITC functionalities simultaneously mounted on the same scaffold increase the activity and/or the ability to hit multiple targets.

From the biological point of view, **2** demonstrated an IC_{50} value in the submicromolar range, more potent than the reference compounds SFN and N-BDMPrNDI, it was the most effective in inducing apoptosis, decreasing mitochondrial potential around 50% in the same range (0.50 μM). Furthermore, **2** was the most potent to activate caspase-8, which can contribute to apoptosis triggering. Finally, it was observed that **2** inhibited the cell growth by blocking the cell cycle in G1 phase.

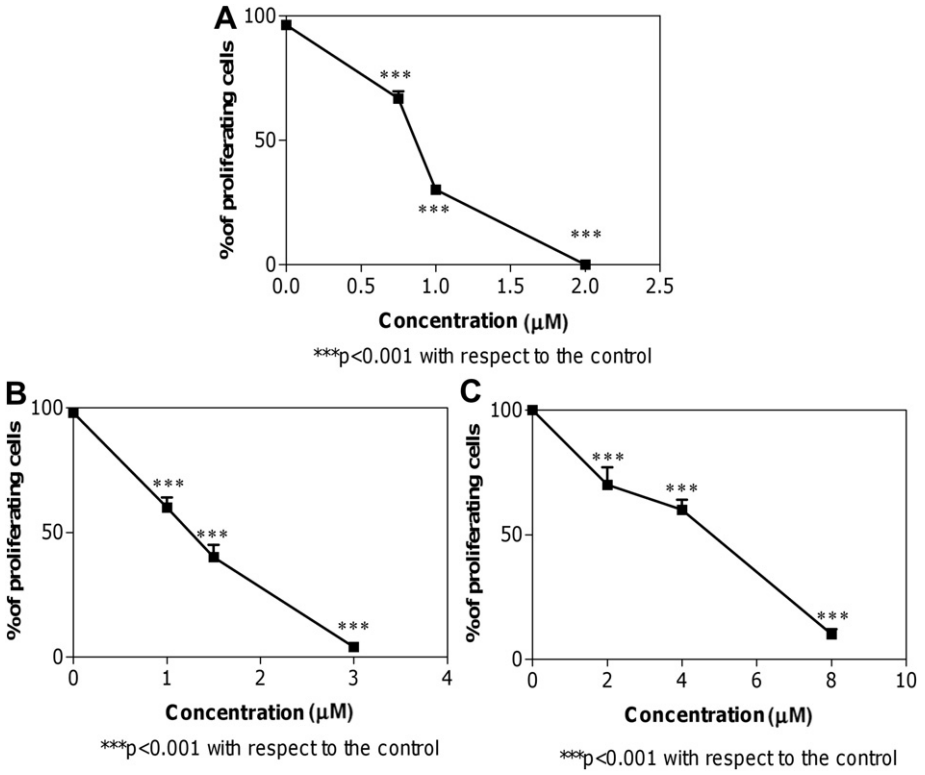

Fig. 6. Inhibition of cell growth after treatment with **2** (A), **1** (B) or **3** (C). Data are means ± SEM of at least three independent experiments.

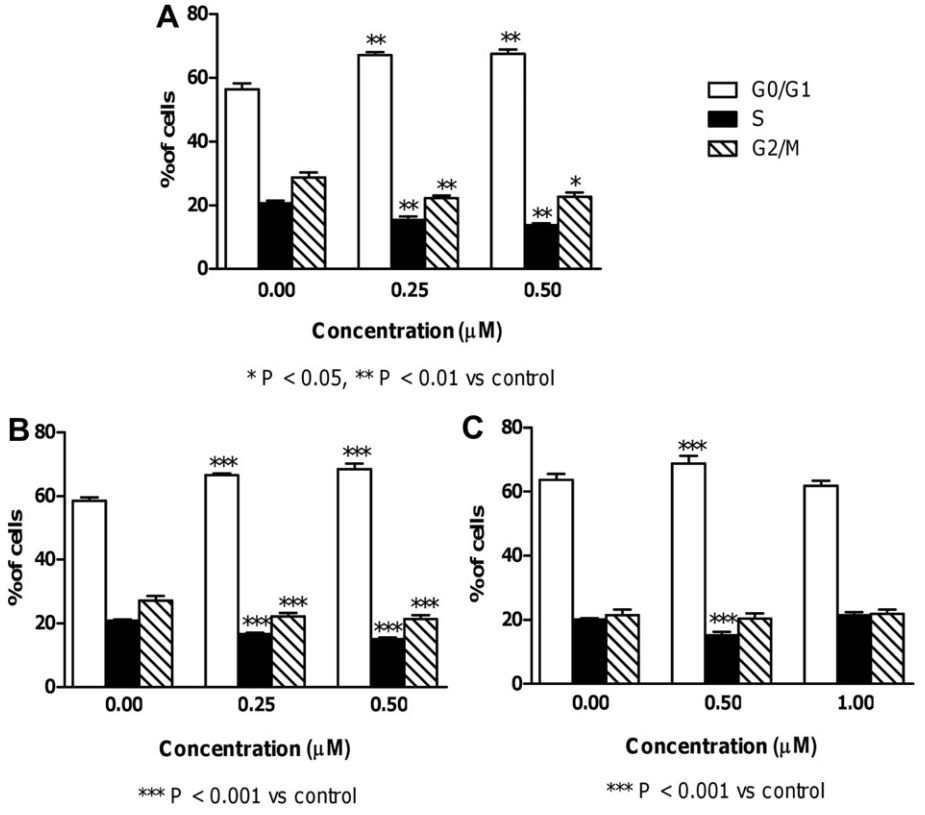

Fig. 7. Cell-cycle distribution following 24 h culture in the absence or presence of **2** (A), **1** (B) or **3** (C). Data are means ± SEM of four independent experiments.

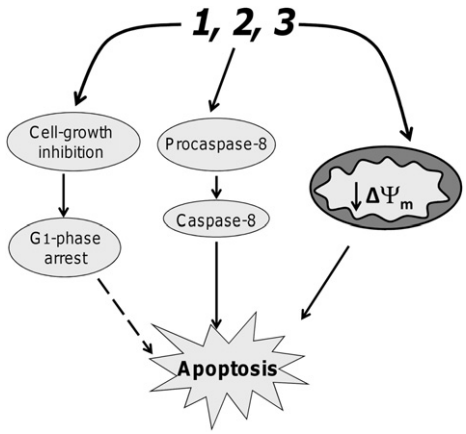

Fig. 8. Proposed anticancer mechanisms of **1**–**3**.

4. Experimental section

4.1. Chemistry

All the synthesized compounds have a purity of at least 95% determined by elemental analysis. Melting point were taken in glass capillary tubes on a Buchi SMP-20 apparatus and are uncorrected. ESI-MS spectra were recorded on Perkin–Elmer 297 and Waters ZQ 4000. ^{1}H NMR and ^{13}C NMR were recorded on Varian VRX 200 and 400 instruments. Chemical shifts are reported in parts per millions (ppm) relative to peak of tetramethylsilane (TMS) and spin multiplicities are given as s (singlet), brs (broad singlet), d (doublet), t (triplet), q (quartet) or m (multiplet) Although IR spectral data are not included (because of the lack of unusual features), they were obtained for all compounds reported, and they were consistent with the assigned structures. The elemental analysis was performed with Perkin Elmer elemental analyzer 2400 CHN. From all new compounds satisfactory elemental analyses were obtained, confirming >95%purity. Chromatographic separations were performed on silica gel columns by flash (Kieselgel 40, 0.040–0.063 mm, Merck) column chromatography. Reactions were followed by thin layer chromatography (TLC) on Merck (0.25 mm) glass-packed precoated silica gel plates (60 F254) and then visualized in an iodine chamber or with a UV lamp. The term "dried" refers to the use of anhydrous sodium sulphate.

4.1.1. General procedure for the synthesis of **1** and **2**

To a solution of **4** [17] and **5** [17] in dry CH_2Cl_2 under nitrogen, 1,1′-thiocarbonyldi-2(1H)-pyridone (in 1:2 M ratio) in dry CH_2Cl_2 was added dropwise and the resulting mixture was stirred at room temperature overnight. The solvent was removed in vacuo and the residue was purified by gravity column using as eluting solvent petroleum ether/CH_2Cl_2/methanol (6/3.5/0.5).

4.1.2. 2,7-Bis-(2-isothiocyanato-ethyl)-benzo[lmn][3,8] phenanthroline-1,3,6,8 tetraone (**1**)

Yellow solid; yield 48%; mp: 209–211 °C ^{1}H NMR (200 MHz, $CDCl_3$) δ 3.97 (t, 4H, J = 6.1), 4.58 (t, 4H, J = 6.3), 8.84 (s, 4H); ^{13}C NMR (100 MHz, $CDCl_3$) δ 40.64, 46.23, 128.28, 128.53, 131.21, 135.77, 163.67; HMRS m/z calcd: 436.0300, found: 436.0311.

4.1.3. 2,7-Bis-(3-isothiocyanato-propyl)-benzo[lmn][3,8] phenanthroline-1,3,6,8-tetraone (**2**)

Yellow oil; yield 41%; ^{1}H NMR (200 MHz, $CDCl_3$) δ 2.17–2.23 (m, 4H), 3.71 (t, 4H, J = 6.5), 4.38 (t, 4H, J = 6.8), 8.81 (s, 4H); ^{13}C NMR (100 MHz, $CDCl_3$) δ 27.51, 37.44, 44.65, 129.32, 131.67, 132.52, 134.46, 162.23; HMRS m/z calcd: 464.0613, found: 464.0601.

4.1.4. {2-[7-(2-Dimethylamino-ethyl)-1,3,6,8-tetraoxo-3,6,7,8-tetrahydro-1H-benzo[lmn] [3,8]phenanthrolin-2-yl]-ethyl}-carbamic acid tert-butyl ester (**6**)

To a mixture of (2-Amino-ethyl)-carbamic acid *tert*-butyl ester and *N*,*N*-dimethylethylenediamine in dry DMF, 1,4,5,8-Naphthalenetetracarboxylic dianhydride was added (molar ratio 1:1:1) and the resulting mixture was refluxed for 2 h. The solvent was removed in vacuo and the resulting residue was purified through flash chromatography using as eluent a mixture of toluene/chloroform/CH_2Cl_2/methanol/33% aq. NH_4OH (4:4:1.5:0.5:0.03) yielding the desired product as yellow oil; 15% yield; ^{1}H NMR (400 MHz, $CDCl_3$) δ 1.22 (s, 9H), 2.35 (s, 6H), 2.67 (t, 2H, J = 6.8), 3.55–3.57 (m, 2H), 4.34 (t, 2H, J = 6.8), 4.38 (t, 2H, J = 5.8), 4.93 (brs, 1H exch with D_2O), 8.72–8.76 (m, 4H); ^{13}C NMR (100 MHz, $CDCl_3$) δ 28.09, 38.55, 38.97, 40.58, 45.66, 56.83, 79.06, 126.30, 126.38, 126.41, 126.49, 130.78, 130.82, 156.06, 162.62, 162.93.

4.1.5. 2-(2-Amino-ethyl)-7-(2-dimethylamino-ethyl)-benzo[lmn] [3,8] phenanthroline-1,3,6,8-tetraone (**7**)

20 ml of HCl 3 N were added to a solution of **6** in 30 ml of methanol and the resulting mixture was stirred overnight at room temperature. Methanol was removed in vacuo and the aqueous phase was washed several times with diethyl ether. The aqueous solution was made basic with K_2CO_3 and extracted with CH_2Cl_2. The organic phase was dried and evaporate to give the title compound as yellow oil; quantitative yield; ^{1}H NMR (400 MHz, $CDCl_3$) δ 1.35 (brs, 2H exch with D_2O), 2.34 (s, 6H), 2.66 (t, 2H, J = 6.6), 3.09 (t, 2H, J = 6.4), 4.27–4.34 (m, 4H), 8.69–8.71 (m, 4H); ^{13}C NMR (100 MHz $CDCl_3$) δ 38.65, 40.30, 43.34, 45.76, 56.92, 126.44, 126.61, 126.66, 130.91, 130.96, 162.77, 163.06.

4.1.6. 2-(2-Dimethylamino-ethyl)-7-(2-isothiocyanato-ethyl)-benzo[lmn][3,8] phenanthroline -1,3,6,8-tetraone (**3**)

To a solution of **7** in dry CH_2Cl_2 under nitrogen, 1,1′-thiocarbonyldi-2(1H)-pyridone (in 1:1 M ratio) in dry CH_2Cl_2 was added dropwise and the resulting mixture was stirred at room temperature overnight. The solvent was removed in vacuo and the residue was purified by gravity column using as eluting solvent CH_2Cl_2/methanol (9/1). The compound was converted into the corresponding *p*-toluensulfonate salt. 45% yield; ^{1}H NMR free base (400 MHz, $CDCl_3$) δ 2.34 (s, 6H), 2.68 (t, 2H, J = 6.8), 3.95 (t, 2H, J = 6.2), 4.34 (t, 2H, J = 6.6), 4.55 (t, 2H, J = 6.2), 8.74–8.79 (m, 4H); ^{13}C NMR (100 MHz, $CDCl_3$) δ 38.68, 39.43, 42.86, 45.76, 56.90, 125.94, 126.71, 126.73, 128.97, 130.90, 141.46, 162.67, 162.74; HMRS m/z calcd: 422.1049, found: 422.1063.

4.2. Biology

4.2.1. Cell cultures

Human Jurkat T leukemia cells were grown in suspension and propagated in RPMI 1640 supplemented with 10% heat-inactivated bovine serum, 1% penicillin/streptomicin solution and 1% L-glutamine solution (all obtained from Sigma, St. Louis, MO, USA). To maintain the exponential growth the culture were divided every third day by dilution to a concentration of 1×10^5 cells/ml. Cells were treated with different concentrations of N-BDMPrNDI, **1**, **2** or **3** prepared from the respective stock solution.

4.2.2. Flow cytometry

All flow cytometric analyses were performed using the easyCyte 5HT (Guava Technologies-Millipore, Hayward, CA, USA).

4.2.3. Cytostatic and cytotoxic activity in vitro

Cells were treated with different concentrations of N-BDMPrNDI, **1**, **2** or **3** for one cell cycle (24 h). Viability was

determined immediately after the end of treatment by flow cytometry. Briefly, cells were mixed with an adequate volume of Guava ViaCount Reagent (containing propidium iodide, Guava Technologies) and allowed to stain 5 min at room temperature. IC_{50} (inhibitory concentration causing cell toxicity by 50% following one cell-cycle exposure) was calculated by interpolation from dose–response curve.

4.2.4. Apoptosis triggering

Cells were treated with different concentrations of **1**, **2** or **3** for 24 h or 72 h. Aliquots of 2×10^4 cells were stained with 100 μl of Guava Nexin Reagent (Guava Technologies), a pre-maid cocktail contained Annexin V-phicoerythrin (Annexin V-PE) and 7-amino-actinomycin D (7-AAD) in buffer, and after a 20 min incubation at room temperature in the dark, the samples were ready for the acquisition. Camptothecin 2 μM was used as positive control.

Active caspase's detection employed an affinity label methodology, using the caspase-8-preferred substrate leucine-glutamic acid-threonine-aspartic acid (LETD) linked to a fluoromethylketone (FMK) moiety, which reacts covalently with the catalytic cysteine residue in the active enzymatic center. A 6-carboxyfluorescein (FAM) group linked to LETD-FMK was used as a reporter. After 24 h of treatment with the three derivatives, cells were stained with 10 μl of freshly prepared 10X working dilution FAM-LETD-FMK (Guava Technologies) (CHEMICON International, Temecula, CA, USA) and incubated for 1 h at 37 °C, protecting tubes from light. After washing, cells were resuspended in 150 μl of 7-aminoactinomycin D diluted 1:200 in 1X working dilution wash buffer (Guava Technologies), incubated for 5 min at room temperature in the dark, and analyzed via flow cytometry. Camptothecin 2 μM was used as positive control.

Mitochondrial potential was evaluated using JC-1 (5,5′,6,6′-tetrachloro-1,1′,3,3′-tetraethylbenzimidazol-carbocyanine iodide), a cationic dye that fluoresces either green or orange depending on mitochondrial potential changes. Cells were treated for 24 h with different concentrations of **1**, **2** or **3**. 200 μl of cell suspension (ca. 1×10^5 cells) were treated with 4 μl of 50X staining solution (Guava Technologies), containing JC-1 and 7-AAD. Samples were incubated for 30 min at 37 °C and analyzed via flow cytometry. Valinomycin 0.09 μM was used as positive control.

4.2.5. Cell-cycle distribution

Cells were treated with different concentration of **1**, **2** or **3** for 24 h, and then fixed with ice-cold ethanol. Samples were then stained with 200 μl of Guava Cell Cycle Reagent (containing propidium iodide), incubated at room temperature for 30 min in the dark, and analyzed via flow cytometry.

4.2.6. Statistical analysis

All results are expressed as mean ± SEM. Differences among treatments were evaluated by one way ANOVA, followed by Dunnett, except for the evaluation of apoptosis performed by Friedman test followed by Dunn's as post test. GraphPad InStat version 5.0 (GraphPad Prism, San Diego, CA, USA) was used for all statistical analysis as well as for IC_{50} value calculation. $P < 0.05$ was considered significant.

Acknowledgment

The authors would like to thank Dr. Nicole Ticchi for technical assistance. Melinda-Rita Marton kindly acknowledges the financial contribution of the Sectorial Operational Programme Human Resources Development 2007–2013 of the Romanian Ministry of Labour, Family and Social Protection through the Financial Agreement POSDRU/88/1.5/S/60203. This research was supported by a grant from MIUR, Rome (PRIN), University of Bologna (RFO), and Polo Scientifico-Didattico di Rimini.

References

[1] B.A. Chabner, T.G. Roberts Jr., Timeline: chemotherapy and the war on cancer, Nat. Rev. Cancer 5 (2005) 65–72.
[2] A.M. Bode, Z. Dong, Cancer prevention research – then and now, Nat. Rev. Cancer 9 (2009) 508–516.
[3] A. Cavalli, M.L. Bolognesi, A. Minarini, M. Rosini, V. Tumiatti, M. Recanatini, C. Melchiorre, Multi-target-directed ligands to combat neurodegenerative diseases, J. Med. Chem. 51 (2008) 347–372.
[4] C.J. Van der Schyf, W.J. Geldenhuys, Polycyclic compounds: ideal drug scaffolds for the design of multiple mechanism drugs? Neurotherapeutics 6 (2009) 175–186.
[5] S. Takenaka, M. Takagi, Threading intercalators as a new DNA structural probe, B. Chem. Soc. Jpn. 72 (1999) 327–337.
[6] M.F. Brana, M. Cacho, A. Gradillas, B. de Pascual-Teresa, A. Ramos, Intercalators as anticancer drugs, Curr. Pharm. Des. 7 (2001) 1745–1780.
[7] R. Martinez, L. Chacon-Garcia, The search of DNA-intercalators as antitumoral drugs: what it worked and what did not work, Curr. Med. Chem. 12 (2005) 127–151.
[8] L.M. Tumir, I. Piantanida, Recognition of single stranded and double stranded DNA/RNA sequences in aqueous medium by small bis-aromatic derivatives, Mini Rev. Med. Chem. 10 (2010) 299–308.
[9] L. Strekowski, B. Wilson, Noncovalent interactions with DNA: an overview, Mutat. Res. 623 (2007) 3–13.
[10] T. Nojima, K. Ohtsuka, T. Nagamatsu, S. Takenaka, Bis-naphthalene diimide exhibiting an effective bis-threading intercalating ability, Nucleic Acids Res. Suppl. (2003) 123–124.
[11] D.A. Gianolio, L.W. McLaughlin, Tethered naphthalene diimide intercalators enhance DNA triplex stability, Bioorg. Med. Chem. 9 (2001) 2329–2334.
[12] S. Balasubramanian, S. Neidle, G-quadruplex nucleic acids as therapeutic targets, Curr. Opin. Chem. Biol. 13 (2009) 345–353.
[13] M. Di Antonio, F. Doria, S.N. Richter, C. Bertipaglia, M. Mella, C. Sissi, M. Palumbo, M. Freccero, Quinone methides tethered to naphthalene diimides as selective G-quadruplex alkylating agents, J. Am. Chem. Soc. 131 (2009) 13132–13141.
[14] M. Nadai, F. Doria, M. Di Antonio, G. Sattin, L. Germani, C. Percivalle, M. Palumbo, S.N. Richter, M. Freccero, Naphthalene diimide scaffolds with dual reversible and covalent interaction properties towards G-quadruplex, Biochimie 93 (2011) 1328–1340.
[15] M. Gunaratnam, S. Swank, S.M. Haider, K. Galesa, A.P. Reszka, M. Beltran, F. Cuenca, J.A. Fletcher, S. Neidle, Targeting human gastrointestinal stromal tumor cells with a quadruplex-binding small molecule, J. Med. Chem. 52 (2009) 3774–3783.
[16] Z.R. Liu, K.H. Hecker, R.L. Rill, Selective DNA binding of (N-alkylamine)-substituted naphthalene imides and diimides to G+C-rich DNA, J. Biomol. Struct. Dyn. 14 (1996) 331–339.
[17] V. Tumiatti, A. Milelli, A. Minarini, M. Micco, A. Gasperi Campani, L. Roncuzzi, D. Baiocchi, J. Marinello, G. Capranico, M. Zini, C. Stefanelli, C. Melchiorre, Design, synthesis, and biological evaluation of substituted naphthalene imides and diimides as anticancer agent, J. Med. Chem. 52 (2009) 7873–7877.
[18] H.J. Schneider, Ligand binding to nucleic acids and proteins: does selectivity increase with strength? Eur. J. Med. Chem. 43 (2008) 2307–2315.
[19] E. Lund, Non-nutritive bioactive constituents of plants: dietary sources and health benefits of glucosinolates, Int. J. Vitam. Nutr. Res. 73 (2003) 135–143.
[20] J.V. Higdon, B. Delage, D.E. Williams, R.H. Dashwood, Cruciferous vegetables and human cancer risk: epidemiologic evidence and mechanistic basis, Pharmacol. Res. 55 (2007) 224–236.
[21] C. Fimognari, M. Lenzi, P. Hrelia, Chemoprevention of cancer by isothiocyanates and anthocyanins: mechanisms of action and structure-activity relationship, Curr. Med. Chem. 15 (2008) 440–447.
[22] F.L. Chung, X.T. Wang, A.J. Di Pasqua, S. Govind, E. McCracken, C. Hong, L.X. Mi, Y.H. Mao, J.Y.C. Wu, Y. Tomita, J.C. Woodrick, R.L. Fine, Selective depletion of mutant p53 by cancer chemopreventive isothiocyanates and their structure-activity relationships, J. Med. Chem. 54 (2011) 809–816.
[23] Y.S. Keum, W.S. Jeong, A.N. Kong, Chemoprevention by isothiocyanates and their underlying molecular signaling mechanisms, Mutat. Res. 555 (2004) 191–202.
[24] C. Fimognari, P. Hrelia, Sulforaphane as a promising molecule for fighting cancer, Mutat. Res. 635 (2007) 90–104.
[25] C. Fimognari, M. Nusse, R. Cesari, R. Iori, G. Cantelli-Forti, P. Hrelia, Growth inhibition, cell-cycle arrest and apoptosis in human T-cell leukemia by the isothiocyanate sulforaphane, Carcinogenesis 23 (2002) 581–586.
[26] C. Fimognari, M. Nusse, M. Lenzi, D. Sciuscio, G. Cantelli-Forti, P. Hrelia, Sulforaphane increases the efficacy of doxorubicin in mouse fibroblasts characterized by p53 mutations, Mutat. Res. 601 (2006) 92–101.
[27] P. Sestili, M. Paolillo, M. Lenzi, E. Colombo, L. Vallorani, L. Casadei, C. Martinelli,C. Fimognari, Sulforaphane induces DNA single strand breaks in cultured human cells, Mutat. Res. 689 65–73.

[28] E. Bertl, H. Bartsch, C. Gerhauser, Inhibition of angiogenesis and endothelial cell functions are novel sulforaphane-mediated mechanisms in chemoprevention, Mol. Cancer Ther. 5 (2006) 575–585.
[29] P. Thejass, G. Kuttan, Antimetastatic activity of sulforaphane, Life Sci. 78 (2006) 3043–3050.
[30] A.K. Sharma, U.H. Sk, A.S.P. Gowda, M.A. Crampsie, J.K. Yun, T.E. Spratt, S. Amin, Development of novel naphthalimide derivatives and their evaluation as potential melanoma therapeutics, Eur. J. Med. Chem. 46 (2011) 3331–3338.
[31] S. Kim, K.Y. Yi, 1,1'-Thiocarbonyldi-2,2'-pyridone – a new useful reagent for functional-group conversions under essentially neutral conditions, J. Org. Chem. 51 (1986) 2613–2615.
[32] A. Eisenfuhr, P.S. Arora, G. Sengle, L.R. Takaoka, J.S. Nowick, M. Famulok, A ribozyme with michaelase activity: synthesis of the substrate precursors, Bioorg. Med. Chem. 11 (2003) 235–249.
[33] N. Khan, F. Afaq, H. Mukhtar, Apoptosis by dietary factors: the suicide solution for delaying cancer growth, Carcinogenesis 28 (2007) 233–239.
[34] S. Moncada, Mitochondria as pharmacological targets, Br. J. Pharmacol. 160 217–219.
[35] S. Salvioli, A. Ardizzoni, C. Franceschi, A. Cossarizza, JC-1, but not DiOC6(3) or rhodamine 123, is a reliable fluorescent probe to assess delta psi changes in intact cells: implications for studies on mitochondrial functionality during apoptosis, FEBS Lett. 411 (1997) 77–82.
[36] S. Fulda, K.M. Debatin, Extrinsic versus intrinsic apoptosis pathways in anticancer chemotherapy, Oncogene 25 (2006) 4798–4811.
[37] M. Malumbres, M. Barbacid, To cycle or not to cycle: a critical decision in cancer, Nat. Rev. Cancer 1 (2001) 222–231.
[38] G.I. Shapiro, J.W. Harper, Anticancer drug targets: cell cycle and checkpoint control, J. Clin. Invest. 104 (1999) 1645–1653.